ELSEVIER

Chemical Engineering Journal 137 (2008) 173–179

Chemical Engineering Journal

www.elsevier.com/locate/cej

Low-pressure synthesis and characterisation of hydroxyapatite derived from mineralise red algae

P.J. Walsh [a], F.J. Buchanan [a], M. Dring [b], C. Maggs [b], S. Bell [c], G.M. Walker [c,*]

[a] *School of Mechanical and Aerospace Engineering, Queens University of Belfast, Belfast BT9 5AG, Northern Ireland, UK*
[b] *School of Biology and Biochemistry, Queens University of Belfast, Belfast BT9 5AG, Northern Ireland, UK*
[c] *School of Chemistry and Chemical Engineering, Queens University of Belfast, Belfast BT9 5AG, Northern Ireland, UK*

Received 18 May 2007; received in revised form 15 October 2007; accepted 16 October 2007

Abstract

There is a great need to design functional bioactive substitute materials capable of surviving harsh and diverse conditions within the human body. Calcium-phosphate ceramics, in particular hydroxyapatite are well established substitute materials for orthopaedic and dental applications. The aim of this study was to develop a bioceramic from alga origins suitable for bone tissue application. This was achieved by a novel synthesis technique using ambient pressure at a low temperature of 100 °C in a highly alkaline environment. The algae was characterised using SEM, BET, XRD and Raman Spectroscopy to determine its physiochemical properties at each stage. The results confirmed the successful conversion of mineralised red alga to hydroxyapatite, by way of this low-pressure hydrothermal process. Furthermore, the synthesised hydroxyapatite maintained the unique micro-porous structure of the original algae, which is considered beneficial in bone repair applications.

Keywords: Hydroxyapatite; Tissue engineering; Bone repair

1. Introduction

Bone repair in particular bone mineralisation presents unique challenges and has become the "target" for many new therapeutic strategies. An aging population, coupled with trauma injuries and bone diseases, could benefit greatly from improved therapeutics, with their own etiologies and therapeutic obstacles [1]. There are currently a wide variety of conventional and contemporary bone repair treatments available, each with inherent advantages and disadvantages. However, despite the enormous benefits brought by these methodologies, the need for bone repair and regeneration with minimal morbidity and mortality remains unexploited [2].

A global demographic shift in population has intensified the need to provide not just replacement therapies but improved long-term cost-effective regeneration solutions [3]. In fact, it is estimated that osteoporosis alone, costs the UK National Health Service £1.7 billion per year [4]. New therapeutic strategies in the form of tissue engineering have the potential to significantly curb healthcare crises, and ultimately, improve the quality of life of millions of patients by revolutionising existing therapies [5].

Calcium-phosphate (CaP) ceramics have received persistent attention as potential substitute material owing to their excellent biocompatibility [6,7]. The main constituent of bone is primarily in the form of hydroxyapatite [Ca_{10} $(PO_4)_6$ $(OH)_2$; HA] accounting for approximately 75% of bone tissue by weight (50% by volume). This is subject to variation with age, anatomical location, general health, and nutritional status [8]. The crystal structure of HA makes it an ideal candidate for replication, as it lends itself to ionic substitution. This is useful when manipulating the resorbability of an implant to ensure its resorption rate is synchronised with the ossification of new bone. In its pure state, the resorption rate of HA is much slower than natural bone. The addition of magnesium ions into its crystal structure improves the materials solubility, giving it a resorption rate similar to natural bone [9].

Several approaches have been taken to develop methods for processing HA, using both natural and synthetic materials. Hydrothermal synthesis [10–15] has been widely investigated, particularly in relation to the conversion of phytogenic calcium carbonate material. Roy and Linnehan [10] successfully converted coral to HA using high pressure and tempera-

* Corresponding author. Tel.: +44 28 9097 4172; fax: +44 28 9097 4627.
E-mail address: g.walker@qub.ac.uk (G.M. Walker).

1385-8947/$ – see front matter © 2007 Elsevier B.V. All rights reserved.
doi:10.1016/j.cej.2007.10.016

Nomenclature

L	percentage mass loss on ignition
M_0	weight of algae pre-heat (g)
M_X	weight of algae after ignition at 550 °C (g)
M_Y	weight of algae after ignition at 1000 °C (g)
X	degree of conversion expressed as a percentage
W	weight of algae at time t (%)
W_0	initial weight of algae sample (g, %)
W_r	residual weight of algae at end of thermal decomposition (%)

ture (103 MPa; 270 °C). The hydrothermal synthesis (Eq. (1)) allowed ionic exchange without destroying the skeletal morphology of the coral/starfish [10].

$$10CaCO_3 + 6(NH_4)_2HPO_4 + 2H_2O \rightarrow Ca_{10}(PO_4)_6(OH)_2 + 6(NH_4)_2CO_3 + 4H_2O + 4CO_2 \quad (1)$$

Other approaches have been described in the literature, including microwave irradiation [16,17], and mechanochemical-hydrothermal synthesis [18].

CaP ceramics derived from coral and sea urchin spines, are gaining more acceptance for orthopaedic use in non-load bearing applications [19]. The advantage of using natural sources of $CaCO_3$ for bone repair is primarily for its unique morphology. These materials have high surface areas which help improve the solubility of the implant and facilitates cellular activity. Some coral species have a similar pore size and porosity to bone. For example, *Goniopora* used to manufacture Pro-Osteon™ has a typical pore size of 500 μm, which is similar to that of cancellous bone [20]. This high macroporosity structure provides an ideal environment to support bone mineralisation. However, the harvesting of coral reefs can have a detrimental impact on marine ecology, and for this reason its widespread use must remain limited.

Recent studies have investigated the use of mineralised red algae, as an alternative to coral [12]. Some of these species have a relatively short growth rate of 2.2 mm/month in optimal (12–18 °C) water conditions [21]. However, these species have the potential to be farmed specifically for commercial use, making it more attractive as a source material. A perceived disadvantage of using algae is its small pore size of >10 μm. Early studies concluded that pores >250 μm induced fibrovascular growth opposed to the differentiation of osteoblastic bone cells [19–22]. More recent *in vitro* studies carried out by Turhani et al. [23,24], have shown that Algipore® with a pore size of 5–10 μm supports attachment and proliferation of osteoblastic type cells. Algipore® is hydroxyapatite derived from a mineralised red algae (*Corallina officinalis*) using high-pressure hydrothermal synthesis similar to the method described by Roy and Linnehan [10]. In addition a study by Roy et al. [25] investigating the use of meso-porous ceramic material concluded they significantly improved the percentage of new bone formation when compared to non-porous ceramic material.

Several synthetic alternatives CaP ceramics have also been development in recent years. These include a range of β-tricalcium phosphates (β-TCP), such as Chronos® and Ceros®, with a typical pore size of 100–500 μm. The use of these synthetic materials has proven problematic in terms of structure and mechanical integrity, limiting their use in orthopaedic applications [19,26].

This study aims to investigate the potential of converting mineralised red alga into a biphasic CaP ceramic by way of low-temperature synthesis. Furthermore, the ability to maintain the algae's morphology, throughout chemical processing is fundamental to its *in vivo* success. *C. officinalis* was selected for this study. The advantages to using this alga were (1) recent studies [23,24] have proven it biocompatibility, (2) it has a favourable morphology, (3) it is a magnesium rich calcite and (4) it is readably available. It was hypothesised that the presences of magnesium in the alga would induce tricalcium phosphate in the resultant material. Furthermore, low-pressure temperature synthesis would help retain the original morphology of the algae. The method purposed herein offers a simple, ambient temperature/pressure alternative to the usual high pressure-temperature synthesis techniques.

2. Materials and methods

2.1. Materials and synthesis

C. officinalis collected from Fanad, Co. Donegal, Ireland, was used for this study. The algae was rinsed in a high-pressure wash until the waters ran clear and dried at room temperature for 24 h. It was then mechanically sieved to a particles size in the range of 1.0–1.4 mm. A thermal heat treatment was used to burn off organic material. This was undertaken in an *Elite* box furnace BRF15/5, with a 5-l chamber capacity. Sample weights of between 5 and 10 g were heated in ceramic crucibles. The soak temperature ranged from 650 to 700 °C and was held for a 12 h fixed period. A slow ramp rate of 0.5 °C/min was used prevent decomposition of the alga structure. After heating, the samples were cooled naturally inside the furnace. The processing parameters were predetermined using thermogravimetric analysis (TGA).

For synthesis, a stoichiometric value of ammonium di-hydrogenphosphate ($NH_4H_2PO_4$, 99.9%; Aldrich) was dissolved in distilled water and added to the pyrolised algae. The reaction was carried out in a 1-l reaction flask (under atmospheric pressure), and continuously mixed at a speed of 100 rpm using a mechanical stirrer. The temperature was maintained at approximately 100 °C for 12 h. The pH was regulated (pre-synthesis) within the range of 10.00–11.00 using ammonium hydroxide [NH_4OH; Aldrich, 28% in H_2O] and maintained above 9 throughout processing. The suspension was cooled at room temperature and left in solution overnight. After this period, the filtrate was separated by vacuum filtration. The filtrate was then washed in distilled water. Residual $NH_4MgPO_4{\cdot}H_2O$ was removed using 10% (v/v) acetic acid under agitation. The material was then neutralised by repeated washing and dried overnight at 90 °C.

2.2. Pyrolysis investigations

A "mass loss" investigation was undertaken to determine the optimum processing conditions for the pyrolysis step. All "mass loss" experiments were carried out in a furnace in an air atmosphere. The algae was washed and dried at 90 °C overnight. A mass of 2 g was heated for 24 h in ceramic crucibles at five different temperatures: 60, 105, 450, 550 and 1000 °C. The samples were heating using a ramp rate of 10 °C/min then cooled gradually to room temperature. The mass loss on ignition was determined in accordance's to BS 6463-102:2001 [27]. The samples were prepared as aforementioned then cooled in a desiccator to room temperature. Immediately a sample of 1 g was weighed to an accuracy of 0.001 g, in a platinum crucible. This was heated at 550 ± 5 °C for 1 h, cooled in a desiccator with a constant external air flow and weighed. This was repeated at hourly intervals until a constant mass was achieved, then repeated at 1000 ± 5 °C. The percentage mass loss due to ignition was calculated using Eqs. (2) and (3).

$$L_{550} = \left[\frac{M_0 - M_X}{M_0}\right] \times 100 \quad (2)$$

$$L_{1000} = \left[\frac{M_0 - M_Y}{M_0}\right] \times 100 \quad (3)$$

2.3. Material characterisation

TGA was carried out using Netzsch STA 449 C Jupiter apparatus in nitrogen and air with a flow rate of 0.05 ml/min. The samples were crushed then heated from ambient to 1000 °C with a rate of 10 °C/min. Calibration was carried out using a platinum crucible. This analysis was preformed to monitor the weight loss in the organic phase and thermal behaviour of the algae during calcification. The results were expressed as the fractional weight loss, which was calculated using Eq. (4).

$$X = \left[\frac{W_0 - W}{W_0 - W_r}\right] \quad (4)$$

Powder X-ray diffraction (XRD) was carried out on a Phillips diffractometer, and was used to determine the crystallinity and phase composition of the sample at each stage of processing. The XRD analysis was carried out under Cu Kα (λ = 1.5406 nm) radiation and recorded in the range of $10^\circ \leq 2\theta \leq 60^\circ$ with a step size of 0.02° for 2θ and count rate of 0.0005°/min. The samples were characterised using semi-quantified Rietveld analysis with '*Phillips*' X' Pert High Score Software.

The samples from each stage of processing were further analysed using Raman Spectroscopy to characterise the material, with respect to its chemical composition and molecular structure. An Avalon R2 bench top model was used with a laser excitation of 785 nm, and approximately 100 mW of power.

Scanning Electron Microscopy (SEM) was carried out using a JEOL 6500 FEGSEM to determine the effect of processing on the structure of the alga. For analysis, the samples were sputter coated with gold for analysis using a Fisons Instrument Coater (Polaron SC 502, UK). Before processing image analysis was carried out from these micrographs to determine the mean pore size of the algae. Lucia image analysis software was used.

2.4. Statistical analysis

All experiments were performed in triplicate, unless otherwise specified. One-way analysis of variance (ANOVA) with a post hoc Fisher's PLSD test was applied to the mass loss data using a confidence level of 5%.

3. Results and discussion

3.1. Alga characterisation

The micrographs in Fig. 1 show the morphologic structure of the raw alga. A cross-section of the branch in Fig. 1(a) shows a concentric uniform pore distribution. A section taken parallel with the branch in Fig. 1(b) reveals long tubular canals. The external surface was rough and dimpled. The pore size was calculated from the micrograph in Fig. 1(a) (using Lucia image analysis software). These results are shown in the histogram in Fig. 2. The results show the pore size to be in the range of 7–13 μm, with over 80% of them 9 μm or larger, with a mode at 10 μm. The cell wall thickness was calculated as 1.8 (±0.71) μm and the pore length as 40.12 (±3.32) μm. Microporosity (10–500 μm) and surface roughness play an important

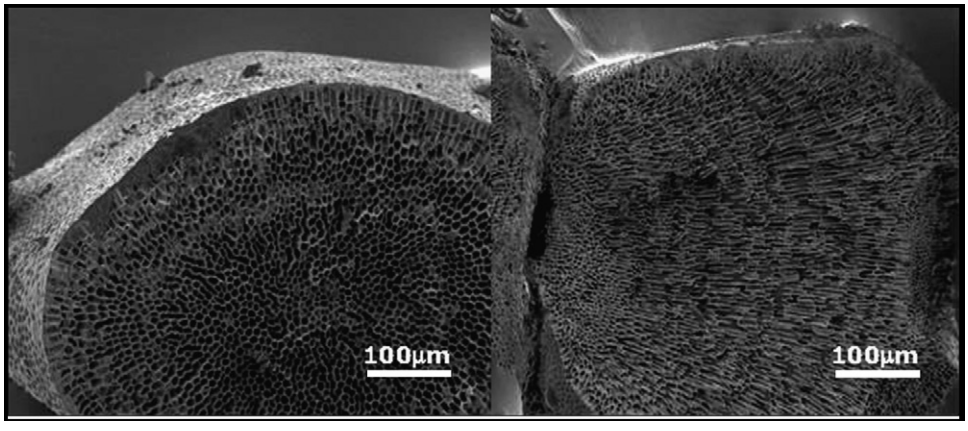

Fig. 1. Micrographs of raw algae internal morphology: (a) perpendicular to pore orientation; (b) parallel to pore orientation.

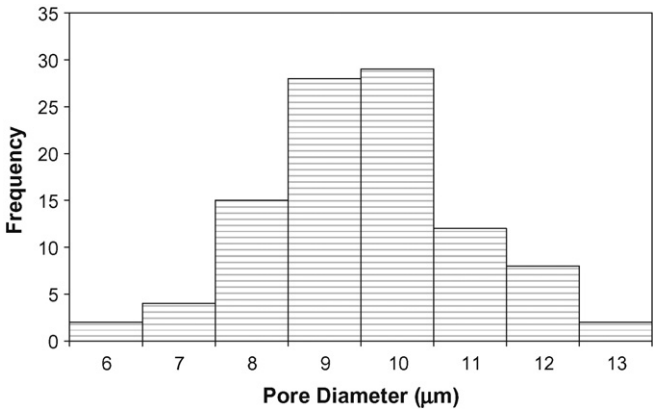

Fig. 2. Histogram of pore size ($n = 100$).

role in osteogensis, as they induce protein adhesion, thus promoting cell attachment and proliferation [28]. In addition, the high porosity increases the algae surface area, which will improve the absorption and bio-resorption properties of the resultant material. Overall, the algae morphology provides some unique and consistent characteristics, which makes a desirable $CaCO_3$ source for bone tissue application.

This unique morphology is a result of the algae calcification process, whereby calcium ions (Ca^{2+}) are precipitated on an organic filament of cells [29]. During hydrothermal conversion a reversal of this process is required as the organic matter can hinder the chemical synthesis by preventing chemical bonding between Ca^{2+}, $CO_3{}^{2-}$, $HPO_4{}^{2-}$ and Mg^{2+}. Removing all the organic material is difficult as it finely distributed and binds the inorganic structure together. In this study a thermal heat treatment was used to burn off the organic material.

3.2. Pyrolysis analysis

To determine the optimum processing conditions for pyrolysis, the decomposition behaviour of the algae was studied using TGA. A non-reactive (N_2) and reactive (air) atmosphere was used to distinguish between (1) the mass loss due to organic decomposition and (2) mass loss due to phase transformation. Fig. 3 shows the degree of carbonate conversion achieved with

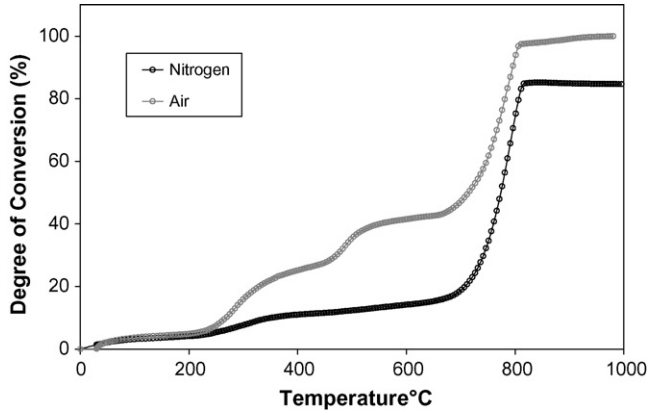

Fig. 3. Degree of "carbonate conversion" of alga under different atmospheres determine by TA.

respect to temperature, calculated from the TGA data. The first stage of decomposition occurs under 220 °C with both gases, whereby chemically bonded water evaporates from the structure. In the next stage, between 220 and 650 °C two different reactions occur. Under N_2 the data tend asymptotically to the maximum degree of conversion. This behaviour signifies the chemical reaction described in Eq. (5). In an air atmosphere the slope of the data shows a higher gradient, as a result of an additional reaction to burn off the organic phase. The difference in mass loss between slopes at 650 °C was 27.1%, suggesting the organic content of the alga was approximately this value. At temperature >700 °C (in both sets of data), the final stage of decomposition occurs, where CO_2 was liberated from the calcite structure, described in Eq. (6). The calculated organic content is in good agreement to those quoted for *C. officinalis* in the literature [30]. Furthermore, the aforementioned pyrolytic behaviour is similar to that reported by Carrasco and Pages, in a study of green alga [31].

$$Mg, Ca(CO_3)_2 \rightarrow CaCO_3 + MgO + CO_2 \quad (5)$$

$$CaCO_3 \rightarrow CaO + CO_2 \quad (6)$$

A pyrolysis experiment was carried out to replicate and further optimise the processing conditions. This was achieved by heating the samples to 550 °C to burn off the organic phase and at 1000 °C to induce complete calcification. The mass loss due to ignition was calculated to be 27.6 (±1.1)% at 550 °C and 58.5 (±1.0)% at 1000 °C. A significant difference in mass loss occurred during the first 8 h of pyrolysis at 550 °C. The mass loss was observed for an additional 4 h to ensure it remained stable. At 1000 °C the mass stabilised during the first hour of pyrolysis, thereafter no significant mass loss was observed. These results were confirmed by a second experiment, whereby the alga was soaked in air continuously for 24 h at 550 and 1000 °C. Other heating regimes have been quoted in the literature to effectively remove organics with temperatures in the range of 400–550 °C, with soak times from 2 to 8 h [32,33]. Therefore, the mass loss at 450 °C was also studied in this experiment. Drying temperatures of 60 and 105 °C were also compared to determine their significant on the mass loss of organics. The mass loss results are reported in Fig. 4. Statistical analysis shows no significance between processing at 450 and 550 °C. At 550 °C a mass loss of 26.5 (±0.9)% was observed, from this <3% corresponds to drying. There was no significant difference in mass loss between the drying temperatures, as indicated in Fig. 4. Heating at 450 and 550 °C produced grey material suggesting the presence of residual carbon. The material was then heated to 650 °C, whereby it was observed to be white. The alga was then treated at 650 °C for different soak periods. The results indicated that mass remained stable at 10 h however had a slight grey discolouration. After 12 h no "grey material" was observed. Temperatures >700 °C resulted in the decomposition of the morphologic structure, and were deemed unsuitable for this application.

XRD was used to determine the effect of heating on the chemical composition of the alga. The results are shown in Fig. 5. A highly crystalline peak was observed in the plot at $2\theta = 30°$ characteristic of $CaCO_3$. Rietveld software analysis

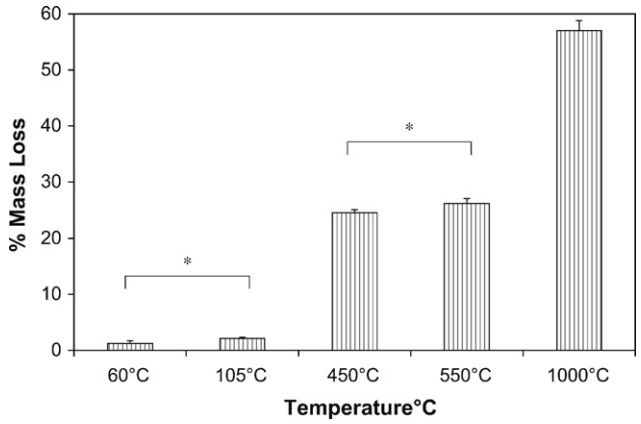

Fig. 4. Pyrolytic behaviour of alga. Error bars represent mean standard deviation for $n = 6$; *<0.5.

confirmed the alga to be a magnesium-rich calcite (Card No. PDF 43–697). A less intense peak was observed at $2\theta = 30^\circ$ after heating at 650 °C signifying the decomposition magnesium from the magnesium-rich calcite structure. The composition at this stage was characterised as 51.1% calcite, 41.9% CaO, 6.6% MgO and 0.4% impurities. At 700 °C a shift in peaks was observed to $2\theta = 38^\circ$ and $2\theta = 54^\circ$, which indicates that the phase transformation to CaO had occurred. The composition was characterised as 74.9% CaO, 9.9% MgO and 4.7% $CaCO_3$.

3.3. Hydrothermal conversion analysis

For the hydrothermal synthesis step within the overall process (as described in Section 2.1), alga pyrolysed at 650 and

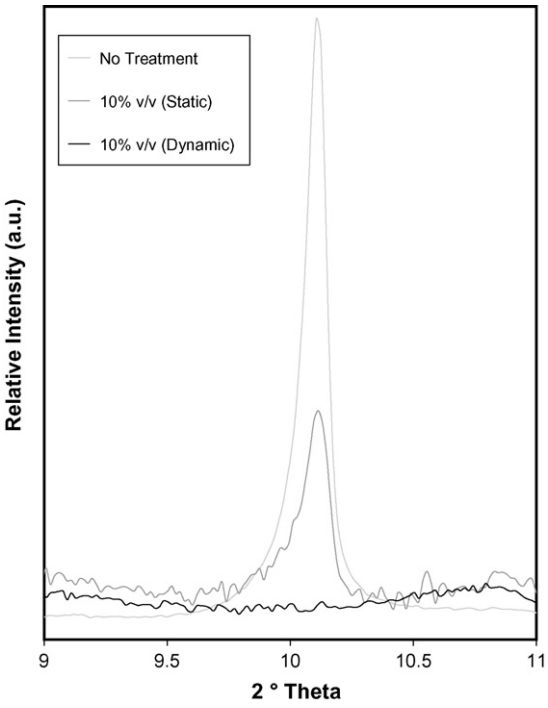

Fig. 6. XRD trace of $(NH_4)Mg(PO_4)\cdot(H_2O)$ peaks after different treatments.

700 °C was used. XRD results indicated that the conversion to hydroxyapatite (HA) had been successful for materials pyrolysed for both temperatures. At 650 °C the resultant material was characterised to be 64% HA, 39% $CaCO_3$ and 3% βTCP. At 700 °C a complete conversion was achieved of 94.8% HA and 4.8% βTCP, with a trace amount of (<0.4%) of SiO_2. How-

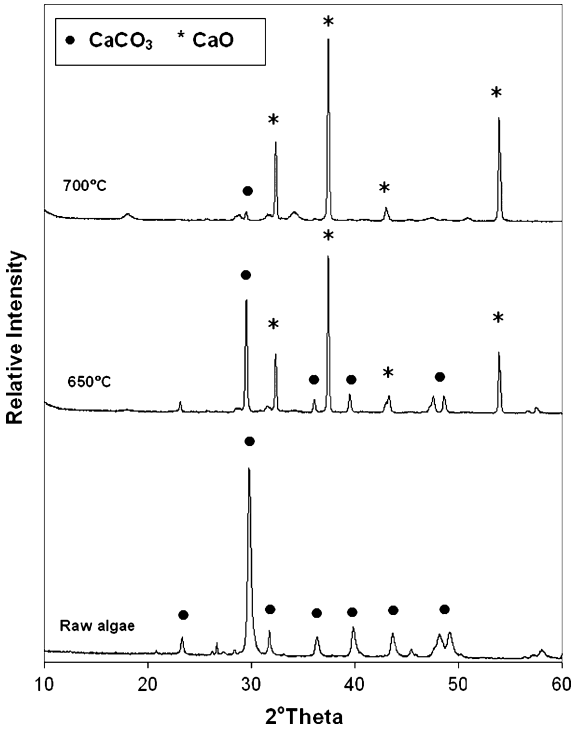

Fig. 5. XRD traces of (a) raw alga (b) after 12 h heat treatment at 650 °C (c) after 12 h heat treatment at 700 °C.

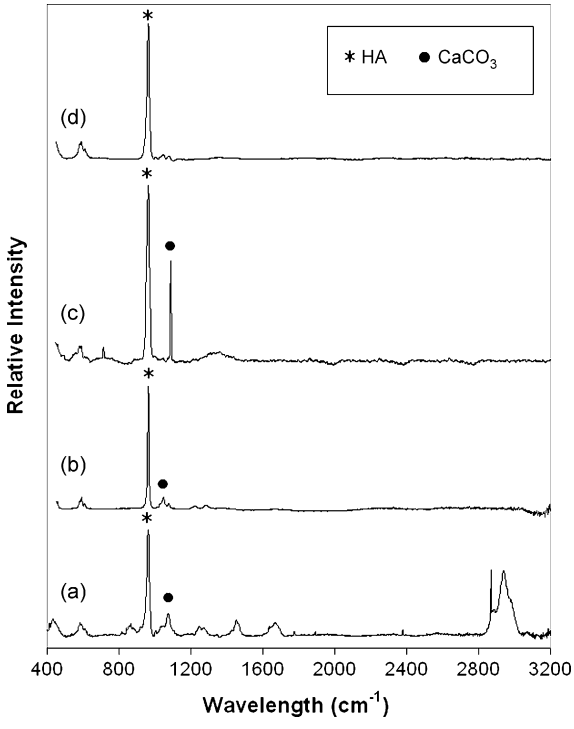

Fig. 7. Raman spectra of (a) freeze dried allograph, (b) Plasma Biotal, (c) corallina HA ($CaCO_3$, 650 °C) and (d) corallina HA ($CaCO_3$, 700 °C).

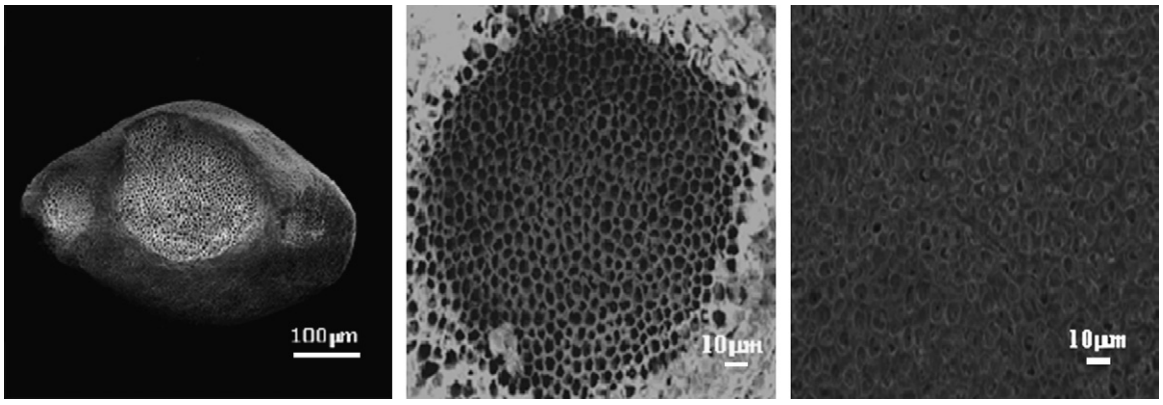

Fig. 8. Micrographs of corallina derived hydroxyapatite after conversion process (perpendicular to pore direction).

ever, the material derived from alga treated at 700 °C was more brittle and less suitable for further processing. Despite the difference in chemical composition, the XRD traces of the materials after hydrothermal synthesis showed no obvious variation with pyrolysis temperature. These results go some way to validating the original hypothesis that the magnesium would induce TCP. The XRD traces in Fig. 6 confirmed that NH_4MgPO_4 was completely removed by a 10% (v/v) acetic wash. A highly crystalline peak was observed at $2\theta = 10^\circ$, which was characteristic peak to NH_4MgPO_4 on the material after processing. After soaking in a 10% (v/v) acetic solution for 24 h a considerable reduction the intensity of this peak was observed. When using the same concentration of acetic acid under static conditions, no peak was observed in the XRD trace suggesting that the residual NH_4MgPO_4 is no longer present.

Raman Spectroscopy was also used to characterise the material post hydrothermal synthesis. In Fig. 7 the processed material was compared to the chemical composition of synthetic HA (Plasma biotal) and freeze-dried allograph bone. In all four spectra a well defined peak at 962 cm^{-1} was detected, which was assigned by the phosphate to oxygen (P-O) vibrations (bending and stretching modes) within the PO_4^{3-} tetrahedral apatite's structure. A second well-defined peak was detected a 1082 cm^{-1}, which was assigned to $CaCO_3$ in the spectra of material processed at 650 °C. These data show good correlation with the XRD results, confirming that HA was produced in this ambient temperature/pressure process.

In the allograft spectra (Fig. 7(a)) broadband peaks (caused by overlapping optical window signals) are observed, which were not visible in the other spectra. The most distinct of these bands was observed at ~2896–2968 cm^{-1}, with other residing ~1222–2000 cm^{-1}, ~1413–1480 cm^{-1} and ~1607–1712 cm^{-1}. These are identified as major collagen bands of different amino acids.

SEM was used to detect changes in the alga structure during processing. The micrograph illustrated in Fig. 8 shows a granule of the material after hydrothermal processing. From the image it is apparent that the structure has remained intact throughout the entire process. The resultant material was granular shaped with a rough external surface that contained open microporous matrix at either end. Image analysis was carried out on the material after synthesis and compared to the raw material in Fig. 9 and

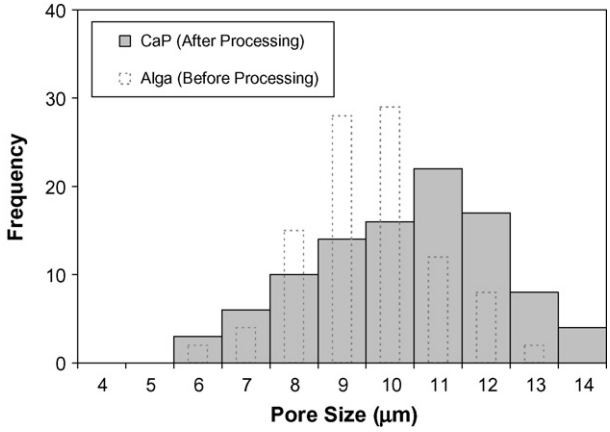

Fig. 9. Histogram of pore size ($n = 100 \times 3$ replicates) for raw alga and alga after chemical synthesis.

Table 1
Statistical data for frequency histograms on pore size (Fig. 9)

Pore Size	Raw alga	CaP
Mean (μm)	10.01	10.72
S.D.	1.37	1.99
Medium (μm)	10.01	11.00
Minimum pore (μm)	6.76	6.52
Maximum pore (μm)	13.58	14.27
Skew	0.22	−0.30

Table 1. The results show a sight increase in the overall pore size. The highest frequency of pores was found to be >9 μm, with a mean pore size of 10.01 μm in the raw material. After processing, a slight shift in mean pore size to 10.71 μm, with a greater maximum pore size of 14.27 μm was observed.

4. Conclusions

The experimental data indicate that the novel processing technique outlined in this work has proven effective in the synthesis of hydroxyapatite in an ambient temperature/pressure hydrothermal process. However, in order to produce HA in the hydrothermal step, attention must be made to: (i) the removal of organic matter; (ii) carbonate decomposition and (iii) mainte-

nance for original alga morphology, in the proceeding pyrolysis step. The overall process produced a material of high purity with good reproducibility in a simple and low-cost technique. The study has shown the potential of using marine algae, processed under low-pressure conditions, to synthesise as more environmentally compatible HA product.

Acknowledgement

This work was partially supported by the European Union funded STREP Project HIPPOCRATES (NMP3-CT-2003-505758).

References

[1] J.E. Shea, S.C. Miller, Skeletal function and structure: implications for tissue-targeted therapeutics, Adv. Drug Deliv. Rev. 57 (2005) 945–957.
[2] L.L. Hench, J.M. Polak, Third-generation biomaterials, Science 295 (5557) (2002) 1014–1017.
[3] P.V. Giannoudis, H.D. Dinopoulos, E. Tsiridis, Bone substitutes: an update, Inj. Int. J. Care Inj. 36S (2005) S20–S27.
[4] E.W.K. Peng, S. Elnikety, N.C. Hatrick, Preventing fragility hip fracture in high risk groups: an opportunity, Postgrad. Med. J. 82 (970) (2006) 528–531.
[5] J. Leor, Y. Amsalem, S. Cohen, Cell scaffolds and molecules for myocardical tissue engineering, Pharmacol. Ther. 105 (2) (2005) 151–163.
[6] D. Tadic, M. Epple, A through physicochemical characterisation of 14 calcium phosphate-based bone substitute materials in comparison to natural bone, Biomaterials 25 (2004) 987–994.
[7] S. Kannan, J.M.G. Ventura, J.M.F. Ferreira, Synthesis and thermal stability of potassium substituted hydroxyapatites and hydroxyapatite/β-tricalciumphosphates mixtures, Ceram. Int. (2006).
[8] J.E. Shea, S.C. Miller, Skeletal function and structure: Implications for tissue-targeted therapeutics, Adv. Drug Deliv. Rev. 57 (7) (2005) 945–957.
[9] B. Tomazic, T.M. Nancollas, Growth of calcium phosphate on hydroxyapatite crystals: the effect of magnesium, Arch. Oral Biol. 20 (1975) 803–808.
[10] D.M. Roy, S.K. Linnehan, Hydroxyapatite formed from coral skeletal carbonate by hydrothermal exchange, Nature 246 (1974) 220–222.
[11] M. Sivakumar, T.S. Sampath Kumar, K.L. Shantha, K. Panduranga Rao, Development of hydroxyapatite derived from Indian coral, Biomaterials 17 (1996) 1709–1714.
[12] G. Felicio-Fernandes, C.M. Laranjeira, Calcium phosphate biomaterials from marine algae. Hydrothermal synthesis and characterisation, Quim. Nova 23 (4) (2000) 441–446.
[13] Y. Xu, D. Wang, L. Yang, H. Tang, Hydrothermal conversion of coral into hydroxyapatite, Mater. Charact. 47 (2001) 83–87.
[14] J. Hu, J.J. Russell, B. Ben-Nissan, Production and analysis of hydroxyapatite from Australian coral via hydrothermal process, J. Mater. Sci. Lett. 20 (2001) 85–87.
[15] S. Jinawath, D. Pongkao, M. Yoshimura, Hydrothermal synthesis of hydroxyapatite from natural source, J. Mater. Sci. Mater. Med. 13 (2002) 491–494.
[16] I. Manjubala, M. Sivakumar, In-situ synthesis of biphasic calcium phosphate ceramics using microwave irradiation, Mater. Chem. Phys. 71 (3) (2001) 272–278.
[17] R. Murugan, K. Panduranga Rao, K. Sampath, Microwave synthesis of bioresorbable carbonated hydroxyapatite using Gonipora, Bioceramics 240–242 (2003) 51–54.
[18] J.M. Oliveira, J.M.R. Grech, I.B. Leonor, J.F. Mano, R.L. Reis, Calcium-phosphate derived from mineralized algae for bone tissue engineering applications, Mater. Lett. 61 (16) (2007) 3495–3499.
[19] D. Green, D. Walsh, S. Mann, R.O.C. Oreffo, The potential of biomimesis in bone tissue engineering: lessons from the design and synthesis of invertebrate skeletons, Bone 30 (6) (2002) 810–815.
[20] K.T. Mahan, M.J. Carey, Hydroxyapatite as a bone substitute, J. Am. Podiatr. Med. Assoc. 89 (8) (1999) 392–397.
[21] H. Tyler-Walters, T. Wiedemann, Coral Weed: *Corallina officinalis*—Basic Information, 2005. [Homepage of *MarLIN*: Marine Life Information Network] [Online]. Available: http://www.marlin.ac.uk/species/Corallinaofficinalis.htm.
[22] Y. Shoufeng, K.F. Leong, Z. Du, C.K. Chua, The design of scaffolds for use in tissue engineering. Part 1. Traditional factors, Tissue Eng. 7 (2001) 679–689.
[23] D. Turhani, B. Cvikl, E. Watzinger, M. Weiβenbock, K. Yerit, M. Thirnher, G. Lauer, R. Ewers, In vitro growth and differentiation of osteoblast-like cells on hydroxyapatite ceramic granule calcified from red algae, J. Oral Maxillofac. Surg. 63 (2005) 793–799.
[24] D. Turhani, E. Watzinger, M. Weiβenbock, K. Yerit, B. Cvikl, R. Ewers, D. Thirnher, In vitro study of adherent mandibular osteoblast-like cells on carrier materials, J. Oral Maxillofac. Surg. 34 (2005) 543–550.
[25] T.D. Roy, J.L. Simon, J.L. Ricci, E.D. Rekow, V.P. Thompson, J.R. Parsons, Performance of degradable composite bone repair products made via three-dimensional fabrication techniques, J. Biomed. Mater. Res. 66 (2) (2003) 283–291.
[26] D. Tadic, M. Epple, A through physicochemical characterisation of 14 calcium phosphate-based bone substitution materials in comparison to natural bone, Biomaterials 25 (2003) 287–994.
[27] BS 6463-102:2001: Quicklime, hydrated lime and natural calcium carbonate.
[28] C. Vitale-Brovarone, L. Verné, E. Robiglio, P. Appendino, F. Bass, G. Martinasso, G. Muzio, R. Canuto, Development of glass–ceramic scaffolds for bone tissue engineering: characterisation, proliferation of human osteoblasts and nodule formation, Acta Biomater. 3 (2) (2007) 199–208.
[29] H.W. Johansen, *Corallina* algae a first synthesis, 1981, p. 144.
[30] S. Marsham, G. Scott, M. Tobin, Comparison of nutritive chemistry of a range of temperature seaweeds, Food Chem. 100 (4) (2007) 1331–1336.
[31] R. Carrasco, P. Pages, Kinetics of the thermal decomposition of green alga ulva by thermogravimetry, J. Appl. Polym. Sci. 93 (2004) 1913–1922.
[32] L.S. Leong, P.A. Tanner, Comparison of methods for determination of organic carbon in marine sediment, Mar. Pollut. 38 (10) (1999) 875–879.
[33] B. Haikali, N. Bendoussan, J.-C. Romano, V. Bousquet, Estimation of photosynthesis and calcification rates of Corallina elongata ellis and solander, 1786, by measurements of dissolved oxygen, pH and total alkalinity, Sci. Mar. 68 (1) (2003) 45–56.